Dielectric spectroscopy investigation for determining the rotational viscosity and the twist elastic constant for the ferroelectric chiral smectic C liquid crystals

2003 J. Phys.: Condens. Matter 15 4671

(http://iopscience.iop.org/0953-8984/15/27/302)

INSTITUTE OF PHYSICS PUBLISHING JOURNAL OF PHYSICS: CONDENSED MATTER

J. Phys.: Condens. Matter **15** (2003) 4671–4677 PII: S0953-8984(03)54305-3

Dielectric spectroscopy investigation for determining the rotational viscosity and the twist elastic constant for the ferroelectric chiral smectic C liquid crystals

J Hmine[1,5], C Legrand[2], N Isaert[3] and H T Nguyen[4]

[1] Laboratoire de Physique de la Matière Condensée, Université Hassan II, FST Mohammadia BP 146, Mohammadia, Morocco
[2] Laboratoire d'Etude des Matériaux et des Composants pour l'Electronique, EA 2601, Université du Littoral-Côte d'Opale BP 717, Calais, France
[3] Laboratoire de Dynamique et Structures des Matériaux Moléculaires, URA no 801, Université de Lille 1, 59655 Villeneuve d'Ascq, France
[4] Centre de Recherche Paul Pascal, Université de Bordeaux 1, 33600 Pessac, France

E-mail: hmine@uh2m.ac.ma

Received 3 October 2002
Published 27 June 2003
Online at stacks.iop.org/JPhysCM/15/4671

Abstract

We present new results of structural, electro-optical and dielectric measurements, concerning the Goldstone mode rotational viscosity and the twist elastic constant in the ferroelectric chiral smectic C (SmC*) phase near an N*–SmA–SmC* multicritical point. This study has been performed on the pure chiral homologue with $n = 11$ from the series of biphenyl alkyloxy benzoates. An Arrhenius behaviour of the Goldstone mode rotational viscosity was obtained and the activation energy was determined for this material. The characteristic parameters are also compared to those obtained for the $n = 10$ compound.

1. Introduction

Liquid crystals exhibiting the chiral smectic C* phase were reported for the first time by Meyer *et al* [1]. Over the last few years, there has been considerable interest in experimental and theoretical studies carried out in efforts to understand the ferroelectric properties of the SmC* phase. Therefore, the helical pitch, tilt angle and spontaneous polarization have been measured as a function of temperature by many researchers for other compounds. However, few studies have been reported in which there is full investigation of the structural, electro-optical and dielectric response of the ferroelectric chiral smectic C*.

In the absence of an external electric field, in the SmC* phase the chirality induces a precession of the direction of the tilt and in-plane spontaneous polarization as there is also

[5] Author to whom any correspondence should be addressed.

Table 1. Chemical formulae, phase sequences and transition temperatures (°C) for the homologues of the biphenyl benzoate series. The meanings of the abbreviations used in this table are: Cr: crystalline phase; Sm: smectic phases A, C*; N*: cholesteric phase; BP: blue phase; I: isotropic phase; •: the phase exists; —: the phase does not exist; ( ): monotropic transition.

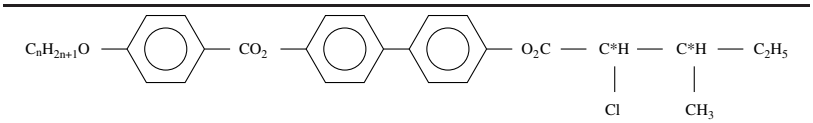

n	Cr		Sm	SmC*		SmA		N*		BP		I
7	•	100	• (52)	•	134	—		•	166	•	166.1	•
8	•	88	—	•	138	—		•	165.5	•	166.5	•
9	•	89	—	•	142	—		•	162	•	162.1	•
10	•	88	—	•	143	•	144	•	159	•	160	•
11	•	88	—	•	146	•	149	•	157	•	157.1	•
12	•	81	—	•	145.5	•	150	•	154	•	154.5	•

precession from one smectic layer to another. This leads to the formation of helicoidal structure with an axis normal to the smectic layers. Thus, the inhomogeneous helical structure means that the macroscopic polarization of the sample vanishes and tends to zero. The helicoidal structure can be deformed by an external electric field applied parallel to the smectic layers (perpendicular to the helical axis). In this case, the dielectric response in the chiral smectic C* phase is governed by four dielectric relaxations [2]. Two of these modes are connected to fluctuations of the polarization, and are called 'polarization modes'. Benguigui [3] has confirmed the presence of these modes for the DOBAMBC compound and has reported high values of the relaxation frequencies of the order of 500 MHz. The other two modes [2, 4, 5] which are connected with the director reorientational motion have relaxation frequencies lower than those observed for the polarization modes. The first of these latter modes is attributed as a Goldstone mode, which corresponds to in-phase fluctuations of the orientation of the tilt direction. This dielectric process has a low relaxation frequency and high amplitude at low temperatures. The second contribution of the response in the SmC* phase is a so-called soft mode, which is due to the fluctuation in the amplitude of the tilt angle. The soft mode appears only at the transition temperature between SmC* and SmA phases, and a few degrees above the transition temperature in the SmA phase. Its amplitude is much lower than that of the Goldstone mode, whereas the relaxation frequency is very much larger than that of the first process.

Using a simple Landau expansion [6], the dielectric strength and relaxation frequency of the Goldstone mode in the SmC* phase can be obtained. The expressions for this relaxation process are linked to the characteristic parameters, namely the twist elastic constant and the rotational viscosity.

In this paper, we will present experimental data for the pure chiral homologue with $n = 11$ from the series of biphenyl alkyloxy benzoates given in table 1. From structural (helical pitch), electro-optical (tilt angle and spontaneous polarization) and dielectric relaxation spectroscopy (dielectric strength and its relaxation frequency), we will show how the Goldstone mode rotational viscosity and twist elastic constant in the SmC* phase can be determined from a combination of a theoretical model and the experimental data. Finally, Arrhenius-type behaviour of the Goldstone rotational viscosity was obtained and the activation energy was estimated. The results are compared with those obtained for the $n = 10$ compound [7, 8].

2. Experimental details

Ferroelectric properties have been studied for the $n = 11$ derivative, showing the phase sequence Cr–SmC*–SmA–N*–BP–I. The synthesis details for this compound from the homologous series ($n = 7$–12) have already been published [7]. The phase assignments and corresponding transition temperatures were determined at atmospheric pressure both by thermal optical microscopy (Mettler F.P.5) and by differential scanning calorimetry (Perkin-Elmer D.S.C. 7). The phase sequences and the transition temperatures of these materials are summarized in table 1.

The helical pitch for the $n = 11$ compound was measured by the Grandjean–Cano method [9, 10] with prismatic planar samples in the N* phase and prismatic complanar (pseudo-homeotropic) samples in the SmC* phase. We can obtain an excellent planar and complanar orientation formed with regular steps in the N* and SmC* phases allowing helical pitch measurements.

We have studied the electro-optical properties of the SmC* phase of this material in the surface-stabilized ferroelectric liquid crystal configuration (SSFLC) [11], including the temperature dependence of the tilt angle (θ), and the spontaneous polarization (P_S). The sample thickness is $\sim$3 μm, estimated by the Newton fringe method. In order to measure the temperature variations of the tilt angle, a low-frequency and high-amplitude electric field ($E = 5$ V μm^{-1}; $F = 0.2$ Hz) were applied to the samples. The spontaneous polarization measurements use the same experimental set-up as the tilt angle; the amplitude of the electric field necessary to saturate the polarization is around 6 V μm^{-1} and its recurrence frequency is about 1 kHz. The reversal of the electric field reverses the polarization. The electric charge transit gives the macroscopic polarization.

The dielectric measurements were made with planar orientation of the sample: the smectic layers are perpendicular to the electrodes in the frequency range 5 Hz–1 MHz—using a previously described experimental procedure [12]. The planar orientation of the sample was achieved with a polyvinyl alcohol (PVA) coating and rubbing. In order to obtain a good alignment, the liquid crystal was put into the cell by capillarity in the isotropic phase. The cell thickness, 30 μm, was chosen much higher than the pitch value to obtain a planar-wound geometry in the SmC* phase. The checking of the sample orientation and the transition temperatures was performed using a polarizing microscope equipped with a heating home stage. The electric field was applied perpendicular to the SmC* helical axis and parallel to the smectic layers. These measurements were made without superimposition of a dc bias on the measurement electric field.

3. Results and discussion

For this compound, the temperature dependence of the pitch is rather classical. Figure 1 gives the pitch variation versus temperature for $n = 11$. In the N* phase far above the N*–SmA transition, the pitch is very short: $p \sim 0.24$ μm, and gives coloured light-selective reflection. On cooling, the N* pitch grows regularly near the SmA phase and diverges at the N*–SmA transition.

In the SmC* phase, the pitch is relatively low far below T_C: $p \sim 1.2$ μm, and increases to 2.2 μm when the temperature increases. Close the SmC*–SmA phase transition, the Grandjean–Cano defects may become invisible because the rotator power cancels with the tilt angle. The 'flat-drop' method [13] has been used and gives the limit value of the pitch ($p \sim 1.4$ μm) at the transition temperature.

In figure 2 we present the evolution of the tilt angle and spontaneous polarization with temperature for $n = 11$. As one can see, at low temperatures and far from the SmC*–SmA

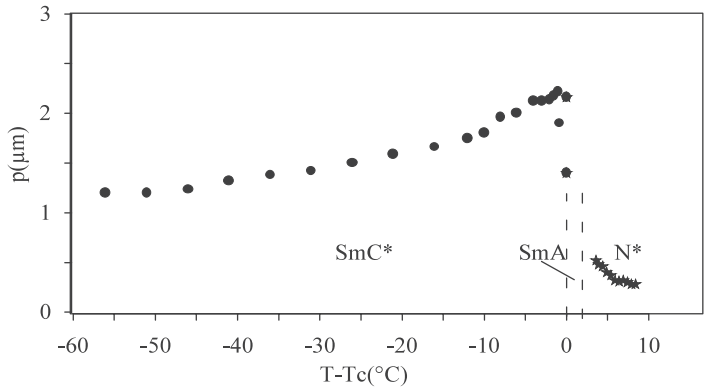

Figure 1. The pitch temperature dependence in the SmC* and N* phases for $n = 11$.

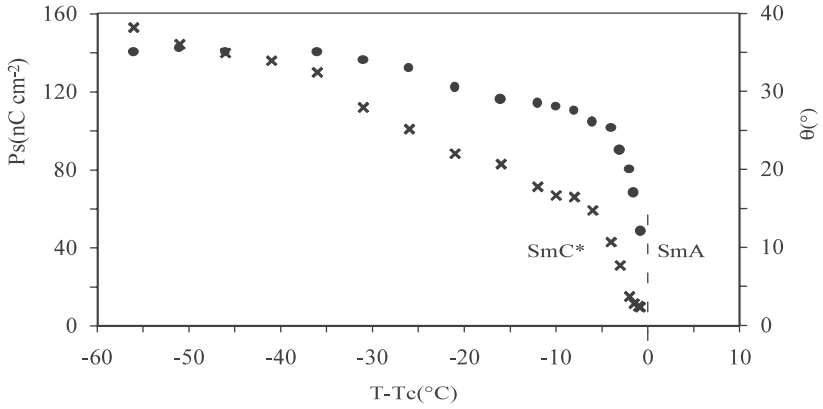

Figure 2. The tilt angle (●) and spontaneous polarization (×) temperature dependences for $n = 11$.

transition, the saturate tilt angle of 35° was measured. When the temperature is increasing, this angle is decreasing roughly at the SmC*–SmA transition temperature, where it is almost equal to 10°, due to the electroclinic effect. The resulting temperature for the spontaneous polarization obtained for $n = 11$ shows that our compounds have a high spontaneous polarization at low temperatures; for instance we obtained, at $T_C - T = 50\,^{\circ}\mathrm{C}$, 160 and 150 nC cm^{-2} respectively for the $n = 10$ [7] and $n = 11$ compounds. This parameter is proportional to the tilt angle and decreases with approach to the SmA phase.

For the dielectric measurements without a dc bias, for this compound the dielectric spectra display one relaxation domain in the SmC* phase. This mechanism process can be eliminated by unwinding the helicoidal structure under dc bias, and connected to the classical Goldstone mode. Figure 4 gives the dielectric amplitude $\Delta\varepsilon_G$ and its critical relaxation frequency (f_G) variations versus temperatures obtained in the SmC* phase. At lower temperatures and far from the SmC*–SmA phase transition, the dielectric strength and the relaxation frequency for this material are rather temperatures independent and have relatively high values: $\Delta\varepsilon_G = 170$ and $f_G = 2$ kHz. At $T = T_C$, the dielectric strength decreases to reach $\Delta\varepsilon_G = 160$, whereas the critical frequency increases to a fairly high value: $f_G = 3.7$ kHz. There is an abrupt increase of f_G close to the SmC*–SmA transition due to the soft-mode contribution, which became predominant at T_C.

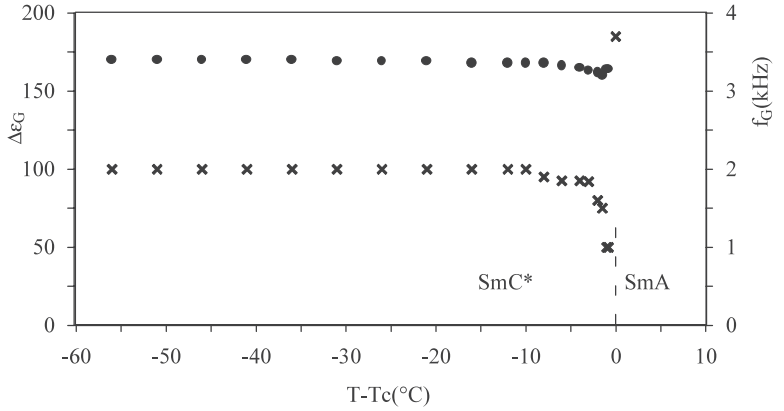

Figure 3. Dielectric strength (●) and relaxation frequency (×) temperature dependences of the Goldstone mode in the SmC* phase for $n = 11$.

From structural, electro-optical and dielectric data, using the theoretical model [6] of the SmC*–SmA phase transition, we can estimate some characteristic parameters for this material. The dielectric strength and the relaxation frequency of the Goldstone mode in the SmC* are given by

$$\Delta\varepsilon_G = \frac{2\pi}{K_{33}q^2}\left(\frac{P_S}{\theta}\right)^2 \tag{1}$$

$$f_G = \frac{K_{33}q^2}{2\pi\gamma_G}. \tag{2}$$

In these equations P_S is the polarization, θ is the tilt angle, $q = 2\pi/p$ is the wavevector of the helicoidal modulation in the SmC* phase, while K_{33} and γ_G are respectively the twist elastic constant and the Goldstone rotational viscosity.

From these equations, we can derive the following expression:

$$\gamma_G = \frac{1}{\Delta\varepsilon_G\, f_G}\left(\frac{P_S}{\theta}\right)^2. \tag{3}$$

From equation (3), and from the experimental values of the polarization, tilt angle, dielectric strength and the relaxation frequency of the Goldstone mode, we can evaluate the Goldstone rotational viscosity γ_G of the SmC* phase. From equation (1), we can deduce the twist elastic constant:

$$K_{33} = \frac{p^2}{2\pi\ \Delta\varepsilon_G}\left(\frac{P_S}{\theta}\right)^2. \tag{4}$$

We thus see that we can also estimate the elastic constant K_{33} of the SmC* phase from the measured values of the helicoidal pitch. From this equation, we can note that the twist elastic constant is closely related to the helical pitch. From the experimental data presented in figures 1–3, we have estimated the elastic constant K_{33} and the rotational viscosity γ_G of the SmC* phase by using equations (4) and (3) respectively. The temperature dependence of these parameters thus obtained for $n = 11$ is shown in figure 4. We obtained, at $T_C - T = 10\,^\circ$C, $K_{33} = 2.3 \times 10^{-11}$ N, $\gamma_G = 40$ mPa s and 5.5×10^{-11} N, 52 mPa s respectively for $n = 10$ [7] and $n = 11$. These values are in good agreement with those obtained by Gouda *et al* [14] and Levstik *et al* [15] for other materials.

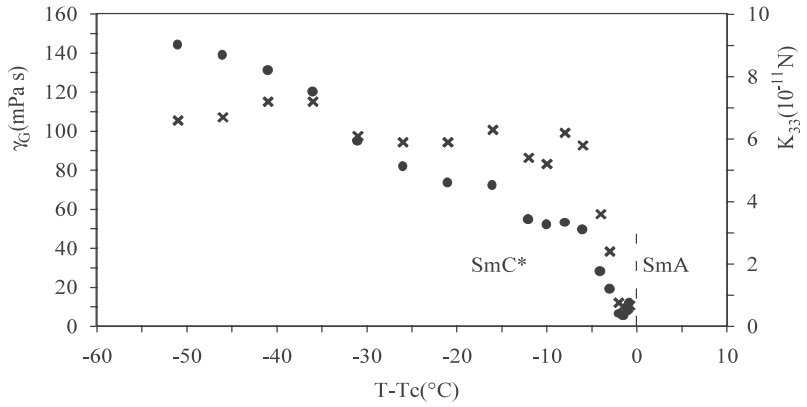

Figure 4. Experimentally determined temperature dependences of the Goldstone mode viscosity γ_G (●) and the twist elastic constant K_{33} (×) in the SmC* phase for $n = 11$.

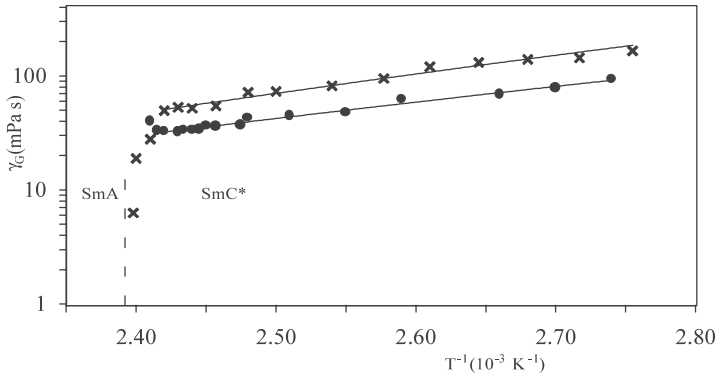

Figure 5. An Arrhenius plot of the experimentally determined rotational viscosity of the Goldstone mode for $n = 10$ (●) and $n = 11$ (×).

We can also note that the temperature dependence of the Goldstone rotational viscosity γ_G in the SmC* phase except near the SmC*–SmA transition obeys the Arrhenius law

$$\gamma_G = \gamma_0 \exp\left(\frac{E_a}{k_B T}\right) \tag{5}$$

where E_a is the activation energy of this mechanism and k_B is the Boltzmann constant.

In figure 5, we show the reverse temperature $1/T$ dependence $\ln \gamma_G \sim E_a/(k_B T)$ of the rotational viscosity obtained for the two homologues: $n = 10$ and 11. Far from the SmC*–SmA phase transition, we can observe a linear behaviour versus reverse temperature. The slopes of the Arrhenius plots give the activation energy values of both materials. We determined the same order of magnitude for the activation energies of this process in the SmC* phase: $E_a = 0.32$ eV for $n = 10$ and 11. Our evaluated values of the activation energies compare well with the values found by other authors using the same methods [15].

4. Conclusions

In this work, we have presented a dielectric method of determining the elastic constant K_{33} of the SmC* phase from the measured values of the helicoidal pitch, which is obtained by

the Grandjean–Cano method. On the other hand, from the experimental values from the tilt angle, spontaneous polarization and dielectric spectroscopy studies (dielectric strength and its relaxation frequency), we evaluated the rotational viscosity γ_G of the Goldstone mode in the SmC^* phase. The activation energy was also determined by assuming Arrhenius behaviour of the Goldstone rotational viscosity.

References

[1] Meyer R B, Liebert L, Strzelecki L and Keller P 1975 *J. Physique Lett.* **36** L69
[2] Blinc R and Zeks B 1978 *Phys. Rev.* A **18** 2
[3] Benguigui L 1982 *J. Physique* **43** 915
[4] Levstik A, Carlsson T, Filipic C, Levstik I and Zeks B 1987 *Phys. Rev.* A **35** 3527
[5] Filipic C, Carlsson T, Levstik A, Zeks B, Blink R, Gouda F, Lagerwall S T and Skarp K 1988 *Phys. Rev.* A **38** 5833
[6] Carlsson T, Zeks B, Levstik A, Filipic C, Levstik I and Blinc R 1990 *Phys. Rev.* A **42** 877
[7] Legrand C, Isaert N, Hmine J, Buisine J M, Parneix J P, Nguyen H T and Destrade C 1992 *J. Physique* II **2** 1545
[8] Hmine J 1991 *PhD Thesis* Université des Sciences et Technologies, Lille 1
[9] Grandjean F 1922 *C. R. Acad. Sci., Paris* **172** 71
[10] Cano R 1968 *Bull. Soc. Fr. Miner. Cryst.* **91** 20
[11] Clark N A and Lagerwall S T 1980 *Appl. Phys. Lett.* **36** 899
[12] Legrand C and Parneix J P 1990 *J. Physique* **51** 787
[13] Brunet M and Isaert N 1988 *Ferroelectrics* **84** 25
[14] Gouda F, Skarp K and Lagerwall S T 1991 *Mol. Cryst. Liq. Cryst.* **209** 99
[15] Levstik A, Kuntnjak Z, Filipic C, Levstik I, Bregar Z, Zeks B and Carlsson T 1990 *Phys. Rev.* A **42** 4